Hydraulic anti-lock‌ʹʦpf anti-skid braking system using fuzzy controller

M. Maghroory[a], A. Farhadi[b,*] and P. Naderi[c]

[a] Department of Electrical Engineering, Tehran, Shahid Rajaee Teacher Training University, P.O.B. 16785136, Iran
[b,*] Department of Mechanical Engineering, Tehran, Shahid Rajaee Teacher Training University, P.O.B. 16785136, Iran
[c] Department of Electrical Engineering, Tehran, Shahid Rajaee Teacher Training University, P.O.B. 16785136, Iran

Abstract

To maintain the stability trajectory of vehicles under critical driving conditions, anti lock-anti skid controllers, consisting of four anti-lock sub-controllers for each wheel and two anti-skid sub-controllers for left and right pair wheels have been separately designed. Wheel and body systems have been simulated with seven degrees of freedom to evaluate the proper functioning of controllers. Anti-lock controllers control brake torque through persistent monitoring of wheels velocity and acceleration and prevent them from locking up by cutting and releasing the brake fluid flow into wheel brake cylinder. On the other hand, anti-skid controllers have been designed in order to maintain the vehicle along a stable trajectory, calculated from the stable spin theory, and to monitor the vehicle's trajectory during braking. This controller maintains the vehicle along the desirable trajectory by monitoring vehicle yaw angle and comparing it with the reference yaw angle, and also by adjusting the level of brake fluid input into each wheel's caliper, and subsequently by adjusting brake torque. At the end of the current research, the use of yaw rate control input in place of yaw angle control input in anti-skid controllers has been suggested through a comparative analysis.

Nomenclature

a_x	Longitudinal acceleration of the vehicle ($^m/_{s^2}$)
a_y	Transverse acceleration of the vehicle ($^m/_{s^2}$)
CG	Vehicle center of gravity
C_x	Longitudinal stiffness of the wheel (N)
C_y	Transverse stiffness of the wheel ($^N/_{rad}$)
F_x	Longitudinal force of the wheel (N)
F_y	Transverse force of the wheel (N)
F_R	Wheel resistive spinning force (N)
F_z	Vertical force exerted on the wheel (N)
h_{cg}	The center of gravity height (m)
I_z	Moment of the vehicle inertia around the z-axis (Kg. m^2)
I_w	Moment of the wheel inertia (Kg. m^2)
L_f	The center of gravity distance from the front axis (m)
L_r	The center of gravity distance from the rear axis (m)

*Corresponding author
Email address: a.farhadi@srttu.edu*

21

M_t	The vehicle total mass (Kg)
R_w	The wheel radius (m)
r	The vehicle yaw rate (rad/s)
r_d	The vehicle desirable yaw rate (rad/s)
T_a	The length of vehicle's axes (m)
T	The torque exerted on wheel ($N.m$)
u	Longitudinal velocity of the center of gravity (m/s)
v	Transverse velocity of the center of gravity (m/s)
x, y	Trajectory coordinate axes (m)
δ	Steering angle (rad)
α	Wheel slip angle (rad)
λ	Longitudinal wheel slip
μ	Wheel friction coefficient
μ_{peak}	The maximum friction coefficient between the wheels and the road
ω	Wheel angular velocity (rad/s)
τ_R	Wheel resistive spinning torque ($N.m$)
τ	Braking torque applied to each wheel ($N.m$)
ψ	Vehicle yaw angle (rad)
ψ_d	Vehicle yaw desirable angle (rad)
F_p	Exerted force on brake pedal (N)
V	The average speed of the four wheels (m/s)
V_s	Vehicle body velocity (m/s)
a_ω	Wheel acceleration ($\mathrm{m}/\mathrm{s^2}$)
a	The distance from the brake pump's rear rod to the pedal junction (m)
b	The distance from the applied force to pedal to pedal junction (m)
g	Gravitational acceleration ($\mathrm{m}/\mathrm{s^2}$)
F_{out}	The applied force to the brake pump's rear rod (N)
$F_{booster}$	Booster force (N)

1. Introduction

Brake systems in modern vehicles are the result of a long-lasting evolutionary process, starting from the first applied hydraulic brake in 1917 [1]. Anti-lock brakes were first utilized in aeroplanes in the 1950s, whose application in the automobile industry was not economical yet [2].

In 1969, the first anti-lock brakes for vehicles were developed by Ford and Kelsey-Hayes Company. However, modern anti-lock brakes with electronic control units were designed and manufactured in 1976 by Daimler-Benz and Bosch [3]. Many suggestions have been offered with respect to the design of anti-lock brakes in multiple articles, in the majority of which intelligent fuzzy controllers and sliding mode controllers have been employed [4-8]. Sliding

mode controllers are very practical in nonlinear systems, and offer good resistance to parameter changes and system disturbances [9].

Naderi et al. [10-13] used sliding mode controllers to design an anti-skid controller. By calculating vehicle yaw angle error, the controller reduced on-the-verge-of-slipping wheels torque and increased other wheels torque. Yet, in practice, it is not possible to increase torque more than it is applied to wheels during braking. Sliding mode controllers were also utilized in the article no. 9 to design an anti-skid controller. However, it was designed and formulated by a set of specific control rules. These rules were implemented through a PID Controller-esque pattern with constant coefficients obtained by trial and error. As a result, these rules are not intelligent or precise enough and do not provide us with the possibility of practical implementation.

Yung et al. [14] proposed an electronic braking system (BBW) to control the yaw angle and unwanted changes in vehicle trajectory on slippery roads. Of the inadequacies of the stated article was the absence of an anti-lock controller alongside the anti-skid controller, which contributes to vehicle yaws and renders them incapable of maintaining their desirable trajectory under hard braking conditions.

In 2013, Naderi & Sharouni [15] compared and contrasted anti-skid sliding mode controllers and BBW ones, pointing to an inadequacy on the part of both in maintaining vehicles desirable trajectory during hard braking conditions as well as in keeping them from yawing, which resulted in locked-up wheels. These inadequacies are fully overcome in the present study by designing an appropriate anti-lock controller.

Among the fuzzy controllers employed for designing anti-lock controllers are neuro-fuzzy controllers [16] and TSK fuzzy model series [17]. Since determining braking pressure using physical sensors is not justified from a security perspective, hydraulic brake systems are utilized in the current study to measure braking pressure in a precise manner. In 2003, Wu & Shih [18] began to develop a mathematical model for hydraulic braking system equations, as well as to implement this system in practice.

In 2012, Nasri et al. [19] presented these equations in a complete manner in the form of equations of state for hydraulic brake systems by taking the effective external parameters on braking systems into account. Through PWM control, Park, Kim and Kim [20] developed an anti-lock brake for air hydraulic brake systems in buses. In 2011, Lin & Song [21] proposed an anti-lock system for hydraulic brakes on trains. Since using motorcycles for transportation purposes are quite common in Asian countries, it is also necessary to develop an anti-lock system for this vehicle [22-28].

The above investigations reveal that, much to our surprise, no effort has been made to incorporate anti-lock brakes into hydraulic brake systems. On the other hand, the designed controllers utilized in more recent studies on anti-lock hydraulic brakes were not intelligent. For instance, to determine the optimum wheel slip rate, predictive control, and Lyapunov equation were used in article no. [29]. In another study, Mirzaeinejad & Mirzaei [30] utilized nonlinear optimization algorithms to prevent vehicle slips on roads with different friction coefficients. As a result, attempts are made in this study to design anti lock-anti skid brakes for hydraulic brake systems using intelligent fuzzy controllers.

This study is organized into six sections. In the first section, the purpose behind the designing of an anti lock-anti skid brake is examined. In the second section, wheels and body are modeled with four and three degrees of freedom, respectively, using Dugoff's nonlinear model. Furthermore, the model for hydraulic brake systems is introduced from brake pedal to wheel cylinder. The third section deals with the design and modeling of anti-lock and anti-skid controllers. The simulation of different braking maneuvers for verifying the desirable performance yielded by the suggested system is the focus of the fourth section. Finally, a general conclusion of the performance of the specified controllers is given.

2. Body, wheel, and hydraulic braking system modeling

Different models have been developed to account for lateral and rotational movements of vehicles with various degrees and complexities.

They are usually identified in terms of the employed degrees of freedom within them. The utilized model in this study is one with seven degrees of freedom. Figure 1 illustrates the vehicle's coordinate system, with x-y being the coordinate system attached to the vehicle and X-Y the coordinate system attached to the earth.

2. 1. Wheel modeling

Based on Dugoff's model, and by applying actuator torque to wheels, wheel motion equations would be as Eq. (1) and (2) [12], [15].

$$I_{wi}\dot{\omega}_i = T_i - R_w F_{xi} - \tau_{Ri} \qquad (1)$$
$$for\ i = fl, fr, rl, rr$$

$$\tau_R = C_0 F_z + C_1 |V_w|^2 \qquad (2)$$

where ω is the wheel angular velocity, T_i is the dynamic torque, τ_R is the resistance torque to the wheel spin, and generally $0.04 \leq C_0 \leq 0.2$ and $C_1 \leq C_0$. Also, F_z is the vertical force exerted on the wheel, and is calculated from Eqs. (3-10) by considering the impact of the body transverse and longitudinal velocity.

$$\mu_i = \mu_{peak,i}\sqrt{1 - A_s R_w(\lambda_i + \tan(\alpha_i))} \qquad (3)$$

$$H_i = \sqrt{\left[\left(\frac{C_x \lambda_i}{\mu_i F_{zi}(1 - \lambda_i)}\right)^2 + \left(\frac{C_y \tan(\alpha_i)}{\mu_i F_{zi}(1 - \lambda_i)}\right)^2\right]} \qquad (4)$$

$$F_{xi} = \begin{cases} \dfrac{C_x \lambda_i}{1 - \lambda_i} & for\ H_i < 0.5 \\[2mm] \dfrac{C_x \lambda_i}{1 - \lambda_i}\left(\dfrac{1}{H_i} - \dfrac{1}{4H_i^2}\right) & for\ H_i \geq 0.5 \end{cases} \qquad (5)$$

$$F_{yi} = \begin{cases} \dfrac{C_y \tan(\alpha_i)}{1 - \lambda_i} & for\ H_i < 0.5 \\[2mm] \dfrac{C_y \tan(\alpha_i)}{1 - \lambda_i}\left(\dfrac{1}{H_i} - \dfrac{1}{4H_i^2}\right) & for\ H_i \geq 0.5 \end{cases} \qquad (6)$$

$$F_{zfl} = \frac{M_t}{(L_f + L_r)}\left[g \cdot \frac{L_r}{2} - a_x \cdot \frac{h_{cg}}{2} + a_y \cdot L_r \cdot \frac{h_{cg}}{T_a}\right] \qquad (7)$$
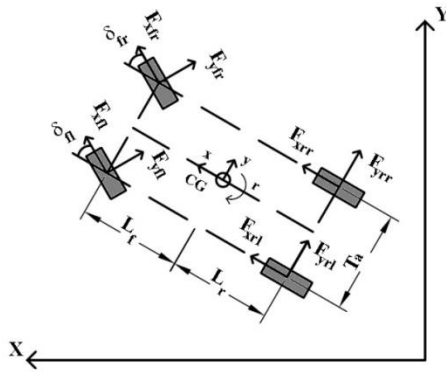
$$F_{zfr} = \frac{M_t}{(L_f + L_r)}\left[g \cdot \frac{L_r}{2} - a_x \cdot \frac{h_{cg}}{2} - a_y \right.$$
$$\left. \cdot L_r \cdot \frac{h_{cg}}{T_a}\right] \tag{8}$$

$$F_{zrl} = \frac{M_t}{(L_f + L_r)}\left[g \cdot \frac{L_f}{2} + a_x \cdot \frac{h_{cg}}{2} + a_y \right.$$
$$\left. \cdot L_f \cdot \frac{h_{cg}}{T_a}\right] \tag{9}$$

$$F_{zrr} = \frac{M_t}{(L_f + L_r)}\left[g \cdot \frac{L_f}{2} + a_x \cdot \frac{h_{cg}}{2} - a_y \right.$$
$$\left. \cdot L_f \cdot \frac{h_{cg}}{T_a}\right] \tag{10}$$

Fig. 1. The vehicle coordinate system.

In Eqs. (3-10), g is the gravitational acceleration, and a_x and a_y are longitudinal and transverse accelerations of the vehicle body's center of gravity, respectively, and are calculated by Eq. (11) and (12) .

$$a_x = \dot{u} - rv \tag{11}$$

$$a_y = \dot{v} + ru \tag{12}$$

In this research, by applying the wheels' longitudinal and transverse forces on the body as input, and calculating longitudinal and transverse dynamics, a three-degree-of-freedom system for the body is achieved. These three degrees are longitudinal velocity, transverse velocity, and vehicle yaw rate shown by u, v, and r, respectively. In this model, the system equations would be as Eqs. (13-16), based on the specified parameters.

$$M_t(\dot{u} - rv) = F_{xfl}cos\delta - F_{yfl}sin\delta$$
$$+ F_{xfr}cos\delta + F_{yfr}sin\delta \tag{13}$$
$$+ F_{xrl} + F_{xrr}$$

$$M_t(\dot{v} + ru) = F_{xfl}sin\delta + F_{yfl}cos\delta$$
$$+ F_{xfr}sin\delta + F_{yfr}cos\delta \tag{14}$$
$$+ F_{yrl} + F_{yrr}$$

$$I_z\dot{r} = L_f[F_{xfl}sin\delta + F_{yfl}cos\delta + F_{xfr}sin\delta + F_{yfr}cos\delta] - L_r[F_{yrl} + F_{yrr}] + \frac{T_a}{2}[F_{xfl}cos\delta - F_{yfl}sin\delta + F_{xfr}cos\delta + F_{yfr}sin\delta + F_{xrl} - F_{xrr}] \tag{15}$$

$$V_s = \sqrt{(u^2 + v^2)} \tag{16}$$

2. 2. Vehicle model

Since brake circuits are separated for front and rear wheels in hydraulic brake systems, a similar kind of design has been separately employed for anti-lock controllers in front- and rear-wheel pairs. By the same token, a similar kind of design has been separately employed for anti-skid controllers in front- and rear-wheel pairs. Figure 2 illustrates the different parts of a hydraulic brake system, including brake booster, the main oil cylinder, and the brake mechanism.

2. 3. Hydraulic brake system model

In a system without any controller, brake fluid would flow directly to the wheel cylinders from the main cylinder during braking; hence accomplishing the braking. The transmission of force from foot to the brake pedal is depicted in Fig. 3.

In Eq. (17), the foot force is magnified by the pedal with a ratio of $\frac{b}{a} = 4.2$, and is transmitted to the main cylinder piston after further magnification [18],[19].

$$F_{out} = \frac{b}{a}F_p \tag{17}$$

Finally, the output force from the booster to the main cylinder is applied according to Fig. 4. Eqs. (18-20) are related to the main cylinder.

$$F_{booster} - A_{mc}P_{mc} - C_{mc}\dot{x}_{mc} - K_{mc}x_{mc} \quad (18)$$
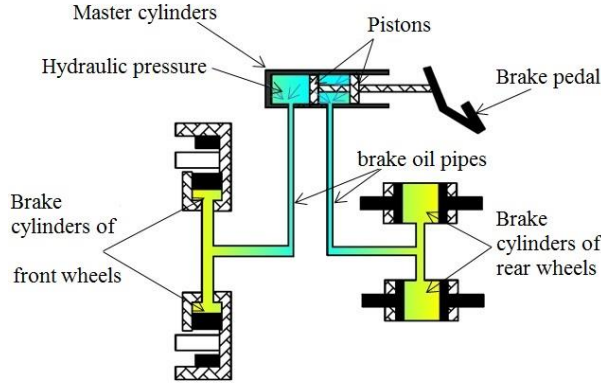$$= M_{mc}\ddot{x}_{mc}$$

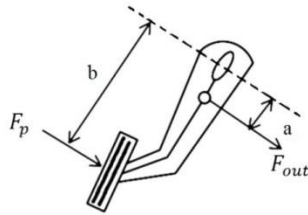**Fig. 2.** The hydraulic brake circuit model without a controller.

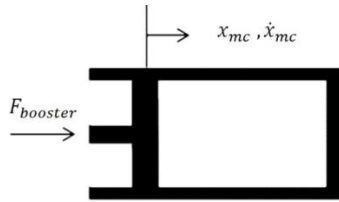**Fig. 3.** The brake pedal model and exerted forces on it.

Fig. 4. The main cylinder model and exerted forced on it.

where $A_{mc}(m^2)$ is the main cylinder cross section, $C_{mc}(Nm/s)$ is the main cylinder damping coefficient, $(N/m)K_{mc}$ is the main cylinder spring stiffness, $(Kg)M_{mc}$ is the main cylinder mass, $P_{mc}(Pa)$ is the internal pressure within the main cylinder, and x_{mc} m is the piston displacement of the main cylinder.

$$P_{mc} = \beta_{mc}\frac{\dot{V}_{mc}}{V_{mc}}$$
$$= \beta_{mc}\frac{A_{mc}\dot{x}_{mc} - Q_{mc} + Q_{wout}}{V_{mc}} \quad (19)$$

$\beta_{mc}(N/m^2)$ refers to the liquid bulk modulus, $Q_{mc}(m^3/s)$ to the oil flow rate discharged from the main cylinder, $Q_{wout}(m^3/s)$ to the oil flow rate from the pump to the main cylinder, and $V_{mc}(m^3)$ to the cylinder volume.

$$Q_{mc} = C_{mc}C_d A_0 \times$$
$$\sqrt{\frac{2}{\rho_0}|P_{mc} - P_{wfl} - P_{wfr} - P_{wrl} - P_{wrr}|} \times \quad (20)$$
$$\text{sign}(P_{mc} - P_{wfl} - P_{wfr} - P_{wrl} - P_{wrr})$$

$C_{mc}C_d$ refers to the main cylinder orifice discharge coefficient in terms of (Nm/s), $A_0(m^2)$ to the main cylinder exit cross section to the brake circuit, $\rho_0 (Kg/m^3)$ to the oil density, and $P_{w(fl,fr,rl,rr)}$ to the wheel cylinder pressure in terms of (Pa).

3. Controller designing

3. 1. The suggested structure for an anti lock-anti skid braking system

The suggested structure for an anti lock-anti skid braking system can be seen in Fig. 5, which consists of six fuzzy controllers, including four anti-lock and two anti-skid sub-controllers. In Fig. 5, three three-phase solenoid valves have been placed on the route of each wheel's brake tubes, receiving commands from anti-lock and anti-skid controllers. As just mentioned, there are three phases to solenoid valves in this system.

• In the first phase, the solenoid valve switches on, causing oil pressure to enter into each wheel's brake circuit directly from the main cylinder.

• In the second phase, the solenoid valve shuts off the brake tube, disconnecting the wheel brake circuit from the main cylinder. This prevents excessive brake pressure when the brake pedal is pressed.

• In the third phase, the solenoid valve reduces the oil pressure within the wheel brake circuit to some extent.

The three stated phases are controlled by anti-lock and anti-skid controllers, with the first two phases pertaining to increase and decrease in

the anti-lock controller pressure, respectively, and the third phase being applicable in reducing brake torque through an anti-skid controller. In Fig. 5, the exerted force on the pedal and the steering angle applied by the driver are identified as system inputs.

The angular velocity of the wheels and its derivative (angular acceleration of each wheel) are utilized as inputs for anti-lock controllers. Yaw error angle, which is obtained by comparing the yaw angle with the desirable yaw angle, and its derivative are utilized as inputs for anti-skid controllers. The outputs for anti-lock and anti-skid controllers are control signals that examine the performance of solenoid valves. Furthermore, they prevent vehicles from locking up and being drifted away from the desirable path by controlling the hydraulic brake fluid flow into the wheels.

3. 2. Hydraulic brake anti-lock system

In this section, the fuzzy model and working principles of anti-lock controllers is discussed.

3. 2. 1. The working principles of anti-lock controllers

The purpose of the braking system is to reduce the braking time and distance, which is accomplished when the maximum friction coefficient between the wheel surface and that of the road is reached for. In addition to the friction coefficient, however, another factor, i.e. slip, is of significance in the braking process, and is defined as the Eq. (21).

$$\lambda = \frac{R_w \omega_i - V_{wi}\cos(\alpha_i)}{V_{wi}\cos(\alpha_i)}; for\ i \qquad (21)$$
$$= fl, fr, rl, rr$$

where λ is the amount of slip between the wheel and the earth, $V_{wi}\cos(\alpha_i)$ is the wheel longitudinal velocity, ω_i is the angular velocity of each wheel, and R_w is the wheel radius.
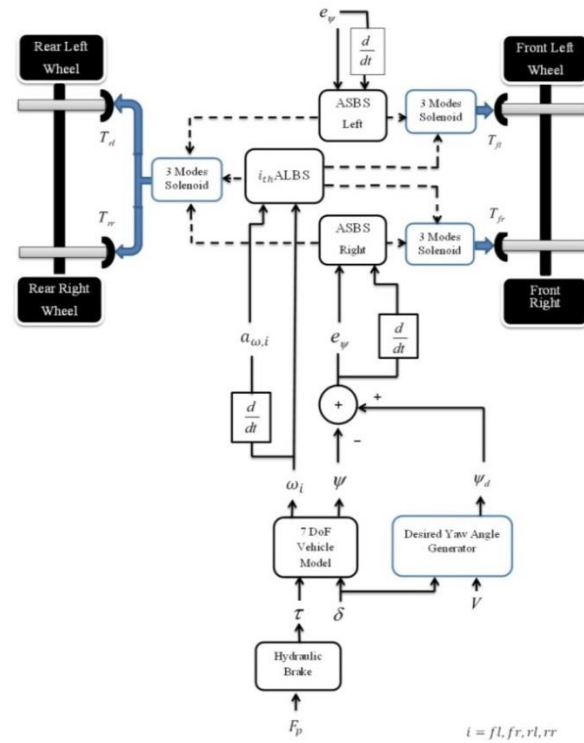

Fig. 5. anti lock (ALBS[1]) – anti skid (ASBS[2]) brake system.

Upon braking, a difference is created in the speed of the wheel and that of the body, and the value of λ becomes restricted to a zero to -1 range. If wheels are locked up, then $\lambda = -1$. The wheel will experience a sharp deceleration just before getting locked up; if the wheel's sharp deceleration process is not controlled it would get locked up before the required stoppage time for the vehicle has been passed. The controller will, then, increase the brake pressure for a second time until the sensor records a sharp reduction in speed. The controller does this task very rapidly before the wheel experiences a drastic change in speed. Consequently, the wheels will decelerate with the same speed rate as that of the vehicle, with the brakes keeping the wheels near the locking point, which allows for the maximum braking force to be applied in the system. Therefore, to prevent wheels from locking up during hard braking conditions, this controller needs to

---

[1] Anti Lock Braking System
[2] Anti Skid Braking System

create an increase as well as a decrease pressure phase.

3. 2. 1. 1. Increase phase

In the increase phase, the oil flow reaches to the wheel cylinder directly from the main cylinder and through the solenoid valve, increasing the wheel cylinder pressure. In Fig. 6 the wheel brake circuit, including the wheel cylinder, brake pads, and wheel disks are illustrated. As is evident from the figure, the oil flow presses the wheel cylinder piston, which in turn presses the pad against the wheel disk, resulting in wheel deceleration and braking.
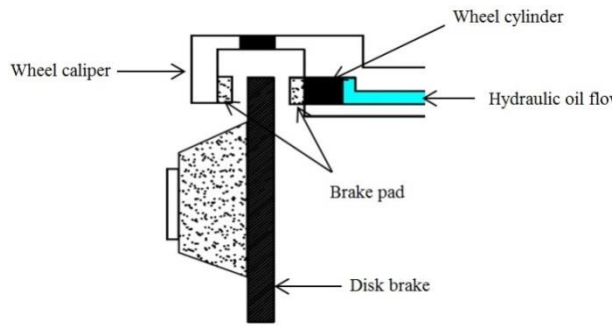

Fig. 6. the wheel brake circuit model.

Equations (22-25) are related to the wheel cylinder piston displacement in the increase phase [18], [19].

$$A_w P_{wfl} - F_{wfl} - C_w \dot{x}_{wfl} - K_w x_{wfl} = M_w \ddot{x}_{wfl} \qquad (22)$$

$$A_w P_{wfr} - F_{wfr} - C_w \dot{x}_{wfr} - K_w x_{wfr} = M_w \ddot{x}_{wfr} \qquad (23)$$

$$A_w P_{wrl} - F_{wrl} - C_w \dot{x}_{wrl} - K_w x_{wrl} = M_w \ddot{x}_{wrl} \qquad (24)$$

$$A_w P_{wrr} - F_{wrr} - C_w \dot{x}_{wrr} - K_w x_{wrr} = M_w \ddot{x}_{wrr} \qquad (25)$$

where A_w (m^2) is the wheel cylinder cross section, C_w (Nm/s) is the wheel cylinder damping coefficient, K_w (N/m) is the wheel cylinder spring stiffness, M_w (Kg) the wheel cylinder mass, $P_{w(fl,fr,rl,rr)}(Pa)$ is the pressure exerted on the wheel cylinder, $F_{w(fl,fr,rl,rr)}(N)$ is the disc reaction force to

the wheel pad pressure, and $x_{w(fl,fr,rl,rr)}(m)$ is the wheel cylinder piston displacement in terms of m. Eqs. (26-29) are related to the generated pressure within four-wheel brake cylinders.

$$P_{wfl} = \beta_w \frac{\dot{V}_{wfl}}{V_{wfl}} = \beta_w \frac{Q_{wfl} - A_w \dot{x}_{wfl}}{V_{wfl}} \qquad (26)$$

$$P_{wfr} = \beta_w \frac{\dot{V}_{wfr}}{V_{wfr}} = \beta_w \frac{Q_{wfr} - A_w \dot{x}_{wfr}}{V_{wfr}} \qquad (27)$$

$$P_{wrl} = \beta_w \frac{\dot{V}_{wrl}}{V_{wrl}} = \beta_w \frac{Q_{wrl} - A_w \dot{x}_{wrl}}{V_{wrl}} \qquad (28)$$

$$P_{wrr} = \beta_w \frac{\dot{V}_{wrr}}{V_{wrr}} = \beta_w \frac{Q_{wrr} - A_w \dot{x}_{wrr}}{V_{wrr}} \qquad (29)$$

where $\beta_w(N/m^2)$ is the liquid bulk modulus, Q_w (m^3/s) is the oil flow rate in the wheel cylinder, and V_w (m^3) is the main cylinder volume. According to Eq. (30), the flow rate input to each wheel cylinder is a quarter of the output flow from the main cylinder.

$$Q_{w(fl,fr,rl,rr)} = \frac{1}{4} Q_{mc} \qquad (30)$$

3. 2. 1. 2. Decrease phase

In the decrease phase, the solenoid valve shuts off the oil flow route from the main cylinder to the wheel cylinder, causing the contained oil within the cylinder to be discharged, re-entering into the brake circuit through pumps. The solenoid valve remains in the decrease phase until the slip value is restored within the allowed range. Equations (31-34) are related to the wheel cylinder piston displacement in the decrease phase [18], [19].

$$F_{wfl} - A_w P_{wfl} - C_w \dot{x}_{wfl} - K_w x_{wfl} = M_w \ddot{x}_{wfl} \qquad (31)$$

$$F_{wfr} - A_w P_{wfr} - C_w \dot{x}_{wfr} - K_w x_{wfr} = M_w \ddot{x}_{wfr} \qquad (32)$$

$$F_{wrl} - A_w P_{wrl} - C_w \dot{x}_{wrl} - K_w x_{wrl} = M_w \ddot{x}_{wrl} \qquad (33)$$

$$F_{wrr} - A_w P_{wrr} - C_w \dot{x}_{wrr} - K_w x_{wrr} = M_w \ddot{x}_{wrr} \tag{34}$$

Due to the loss of oil pressure, and consequently the loss of brake torque in this phase, the disk reaction force pushes the pad back, resulting in oil discharge from the wheel cylinder. Equations (35-38) are related to the wheel cylinder pressure in the decrease phase.

$$P_{wfl} = \beta_w \frac{\dot{V}_{wfl}}{V_{wfl}} = \beta_w \frac{A_w \dot{x}_{wfl} - Q_{woutfl}}{V_{wfl}} \tag{35}$$

$$P_{wfr} = \beta_w \frac{\dot{V}_{wfr}}{V_{wfr}} = \beta_w \frac{A_w \dot{x}_{wfr} - Q_{woutfr}}{V_{wfr}} \tag{36}$$

$$P_{wrl} = \beta_w \frac{\dot{V}_{wrl}}{V_{wrl}} = \beta_w \frac{A_w \dot{x}_{wrl} - Q_{woutrl}}{V_{wrl}} \tag{37}$$

$$P_{wrr} = \beta_w \frac{\dot{V}_{wrr}}{V_{wrr}} = \beta_w \frac{A_w \dot{x}_{wrr} - Q_{woutrr}}{V_{wrr}} \tag{38}$$

Q_{wout} is the oil flow discharged from the wheel cylinder, which is calculated from Eqs. (39-42).

$$Q_{woutfl} = C_w C_d A_0 \sqrt{\frac{2}{\rho_0} |P_{wfl}|} sign(P_{wfl}) \tag{39}$$

$$Q_{woutfr} = C_w C_d A_0 \sqrt{\frac{2}{\rho_0} |P_{wfr}|} sign(P_{wfr}) \tag{40}$$

$$Q_{woutrl} = C_w C_d A_0 \sqrt{\frac{2}{\rho_0} |P_{wrl}|} sign(P_{wrl}) \tag{41}$$

$$Q_{woutrr} = C_w C_d A_0 \sqrt{\frac{2}{\rho_0} |P_{wrr}|} sign(P_{wrr}) \tag{42}$$

Anti-lock fuzzy controllers have two inputs and an output. The first input is the difference between the angular velocity of each wheel and the average angular velocity of the three others at any given moment ($\Delta\omega$). The second input is the angular acceleration of each wheel (a) and the controller output of the difference in pressure to the brake lining with normal pressure for braking without wheels to be locked. Fuzzy controller uses fuzzy rules and changes the controller input to estimate the difference in pressure on the brake lining with ideal pressure and then $\Delta p = p_{ideal} - p_{real}$ is calculated .To improve the accuracy of the control a range of Δp is selected of the small fuzzy controller (shown between 10pa to -10 pa). On the way of the fuzzy output there is a switch that its output shows No. 1 in the case of a positive Δp, otherwise, it shows 0. The switch opens and closes the flow of oil into the cylinder of the wheel brake, and when $\Delta p \geq 0$, it means that the pressure on the brake lining has not still reached the desired phase of braking pressure (output switch = 1); therefore, more pressure should be placed. When $\Delta p < 0$, this means that the optimum braking pressure on the brake lining has increased and the risk of wheel locking has occurred. At this time, output is zero and phase of decreasing the pressure become activated. Therefore, output changes to a digital signal, on the verge of locking wheels. It causes the brake pressure in the wheel brake cylinders to be connected and disconnected. With the start of braking, acceleration and angular wheels will be negative and the range of zero to $-40 \frac{m}{s^2}$ for each wheel angular acceleration is intended as a proper control range (based on trial and error). Therefore, the range of 0 to $-12 \frac{m}{s}$ is considered for an average speed difference of each wheel with the three others. In choosing interval fuzzy function, there are not the same range of spans. The more the velocity and the angular acceleration values are negative, the larger the interval fuzzy function is in order to precisely increase the control in determining the time of connecting and disconnecting the flow of oil braking in the wheels cylinder on the verge of wheels once they are to be locked. The membership functions and rules table for this controller are presented in Fig. 7 and Table 1, respectively.

3. 3. Hydraulic brake anti-skid system

In this section, the fuzzy model and working principles of the anti-skid controller are discussed.

3. 3. 1. The working principles of the controller

To prevent vehicle skid and yaw from the original path, the desirable path should, first, be estimated, and then vehicle yaw be prevented by comparing the actual motion path with the desirable motion path. To this end, the vehicle ideal yaw angle φ_d is first defined.
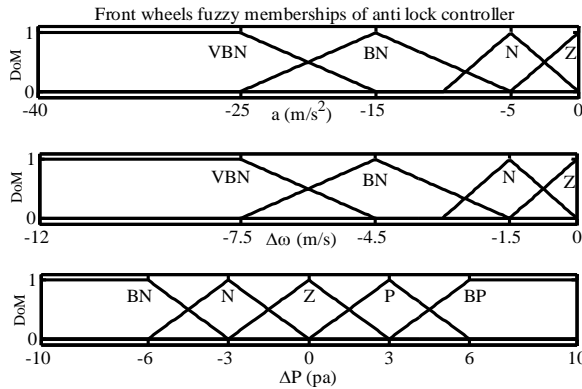

Fig. 7. Membership functions of anti-lock fuzzy controller inputs and output for front wheels.

Table 1. Anti-lock fuzzy controller rules table for front wheels.

a \ $\Delta\omega$	VBN	BN	N	Z
VBN	BN	N	Z	P
BN	N	Z	P	BP
N	Z	P	BP	BP
Z	P	BP	BP	BP

3. 3. 1. 1. The vehicle ideal yaw angle

According to the stable spin theory, vehicle speed and yaw rate r allow for Eqs. (43-46), [10-14].

$$L = L_f + L_r \tag{43}$$

$$A = \frac{M_t}{2L^2} \cdot \frac{L_r C_{y,r} - L_f C_{y,f}}{C_{y,r} C_{y,f}} \tag{44}$$

$$r_d = \frac{1}{1 + AV^2} \cdot \frac{V}{L} \cdot \delta \tag{45}$$

$$\varphi = \int_{t_{start}}^{t_{end}} r \, . \, dt \, , \quad \varphi_d = \int_{t_{start}}^{t_{end}} r_d \, . \, dt \tag{46}$$

r_d is the vehicle desirable yaw rate, φ and φ_d are the vehicle ideal and actual yaw angles, respectively. $C_{y,r}$ and $C_{y,f}$ are lateral stiffness of the front and rear wheels, respectively. t_{end} and t_{start} are the starting and end times of braking, respectively, and V is the vehicle body speed. In vehicles without any controller, wheels change much more rapidly in speed than bodies do, in hard braking conditions. Therefore, the body speed would not be measurable in such situations. However, by preventing the wheel speed from experiencing sudden changes, and subsequently from locking up, anti-lock brakes bring wheel and body speed changes closer to each other in braking situations. It could be stated, therefore, that according to Eq. (47), the body speed is approximately equal to the average linear speed of the four wheels.

$$V = R_w(\omega_{fl} + \omega_{fr} + \omega_{rl} + \omega_{rr})/4 \tag{47}$$

Braking on roads with various friction coefficients, and hard braking situations on road twists are among the most important situations in which vehicles are exposed to skids. At the time of braking, detour occurs when the vehicle brake torque of the sides are not equal. When the two sides of the vehicle wheels experience different friction coefficients, brake torque difference between the side wheels is created. The wheel, which is located on the slippery side has lower braking torque than the other wheels. It should be considered that anti-skid controller finds wheels with high friction coefficient and reduces the braking torque to balance between the torque of the wheels on the car sides by checking the control inputs and identifying the detour of cars. Anti-skid Mamdani type fuzzy controllers have two control inputs: $\Delta\varphi = \varphi_d - \varphi$ which refers to the vehicle yaw angle from the desirable trajectory, and $d(\Delta\varphi)/dt$ which refers to the vehicle yaw rate. The fuzzy controller output, i.e. K, controls the brake fluid flow rate into the wheel brake pad. If the inputs'

changes are insignificant, then $K = 0$, meaning that the controller allows the brake fluid flow to completely penetrate into the brake pad. Otherwise, if the amounts of inputs increase more than a certain extent, K would have a value in the range of $0 - 1$. The input oil flow rate to the wheel cylinder is proportional to the value of K. For instance, if $K = 0.25$, only $3/4$ of the input oil flow would enter into the wheel cylinder. The membership functions and rules table for this controller are presented in Fig. 8 and Table 2, respectively.

In designing anti-skid controllers, an important point is to use an appropriate control input not only to assist in the timely identification of vehicle yaw but to display resistance against rapid changes of road conditions. For instance, if placed on a road, which is initially only slippery on the right-hand side and suddenly the road situation is reversed, i.e. it is only slippery on the left-hand side, and the input should be able to properly identify these rapid changes in road conditions. Therefore, in the simulations conducted in section four, the impact of two inputs, namely, yaw angle and yaw rate, on the controller performance under rapid road condition changes is examined. To achieve this, an anti-skid controller with angle yaw as control input together with its derivative is, first, used, and the process is repeated for the yaw rate as the other control input.

4. Simulation

In this section, each of anti-lock and anti-skid controllers is examined under different maneuvers. The simulations were conducted under MATLAB/Simulink environment. It should be noted that the vehicle initial speed was deemed 120 km/h for all presented maneuvers.

4. 1. The evaluation of anti-lock controller performance

Anti-lock controllers are expected to prevent wheels from locking up when their speed decelerates more rapidly than that of the vehicle; thus assisting drivers in better handling

of vehicles by reducing the braking distance. The performance of an anti-lock controller was studied on a dry-asphalt road, with the friction coefficient of $\mu_{peak} = 1$, a zero steering angle, and a brake pedal force as illustrated in Fig. 9. The wheel slip curve with/without using an anti-lock controller and the exerted brake torque wheel with/without using an anti-lock controller are demonstrated in Fig. 10 and 11, respectively. The braking time and the driver's reaction time for pushing and releasing the brake pedal were assumed 2 and 0.1 seconds, respectively.
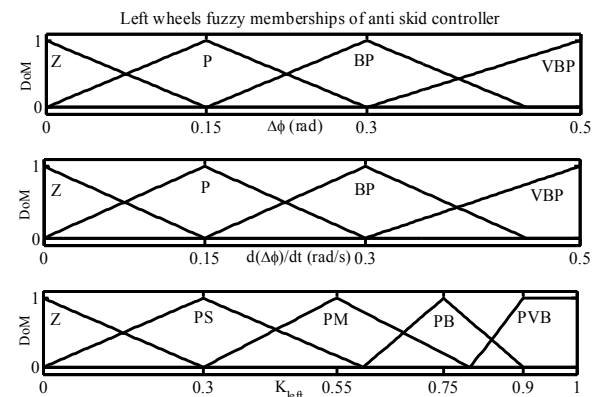

Fig. 8. Membership functions of anti-skid fuzzy controller inputs and output for left wheels.

Table 2. Anti-skid fuzzy controller rules table for left wheels.

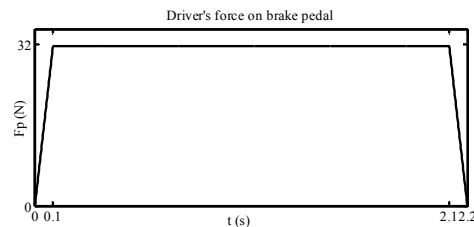| Δr ⟍ $\Delta\varphi$	Z	P	BP	VBP
Z	Z	Z	PS	PM
P	Z	PS	PM	PB
BP	PS	PM	PB	PVB
VBP	PM	PB	PVB	PVB

Fig. 9. The exerted force on the brake pedal.

As can be seen from Fig. 10 and 11, on hard braking conditions with a 32-newton brake pedal force and without using an anti-lock controller, the wheels locked up within less than the first second of braking. Through the proper shutting off and releasing of the braking torque in front and rear wheels, and by maintaining the wheel slip value within the range of $-0.3 \leq \lambda \leq -0.2$, the anti-lock controller prevented the wheels from locking up and the vehicle from yawing, which resulted in a reduced braking distance. Note that the cause of the difference between the curves of the front and rear wheel skid is the difference in the force of weight to the wheels. At the time of braking, the vehicle weight is on the front wheels and therefore front wheels experience friction. Consequently, skid of the rear wheels will be larger.
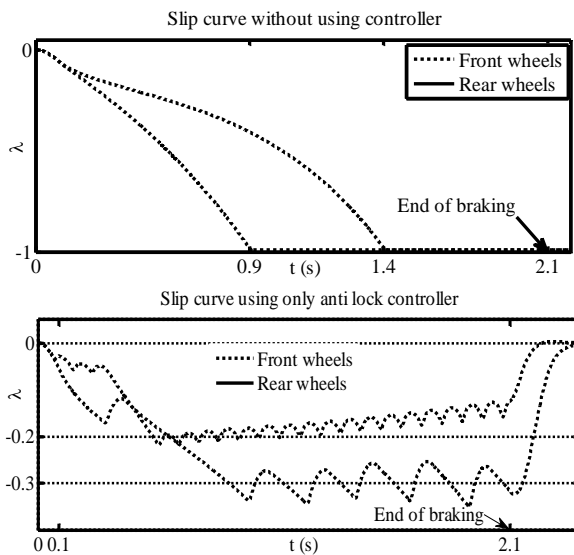

Fig. 10. The wheels slip curves with/without using an anti-lock controller.

4. 2. *The evaluation of anti-skid controller performance*

The anti-skid controller performance should be evaluated alongside its anti-lock counterpart, in that, in case the wheels get locked up, the anti-skid controller would no longer be capable of preventing vehicle yaw. As a complement to the anti-lock controller, the anti-skid controller plays a fundamental role in vehicle control

under critical conditions, such as roads with different coefficients of friction, hard braking situations on road twists, and maneuvers that include multiple direction changes. The controller performance with respect to maintaining the intended vehicle trajectory could be analyzed and evaluated by simulating any of such scenarios.
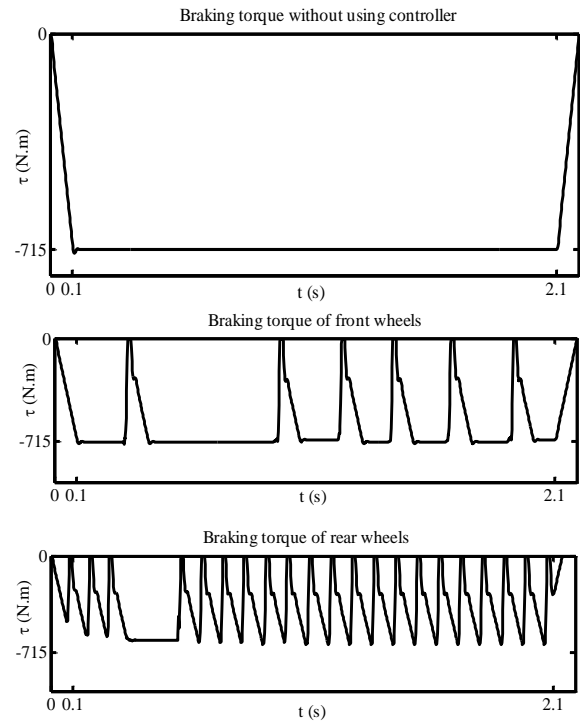

Fig. 11. The wheels torque curves with/without using an anti-lock controller.

4. 2. 1. *Roads with different coefficients of friction*

In this section, the controller performance is evaluated by assuming a zero steering angle and four specified situations in A-D. It is worth noting that the specified situations are consistent throughout the braking process.
Braking [takes place] on a normal road with $\mu_{peak} = 1$ without utilizing any controller; the vehicle trajectory in this situation is taken as the reference trajectory.
Braking on a road with $\mu_{peak} = 1$ for left wheels and $\mu_{peak} = 0.7$ for right wheels, without utilizing any controller.

Braking on a road with $\mu_{peak} = 1$ for left wheels and $\mu_{peak} = 0.7$ for right wheels, using merely a single anti-lock controller.

Braking on a road with $\mu_{peak} = 1$ for left wheels and $\mu_{peak} = 0.7$ for right wheels, using anti-lock and anti-skid controllers (with yaw angle as control input)

Assuming pedal force, an approximate of about 16 Nm simulations of the above situations is done. As seen in Fig. 12, the steering angle in all the maneuvers is zero, the only factor of the vehicle's yaw is the road conditions. Considering the mentioned conditions in every single maneuver, the first one indicates the car is moving in a straight line. In the second one, the vehicle (difference in coefficient of friction of the two sides of the vehicle) is skidded and distracted due to road conditions. In the third one, the anti-lock controller only prevents wheels to be locked, but when the wheels do not lock it can also skid due to the road conditions. Hence, anti-lock controller is an important but not sufficient factor to control the vehicle. At last, in the last situation, anti-lock/skid controllers help the vehicle to go in the right direction.
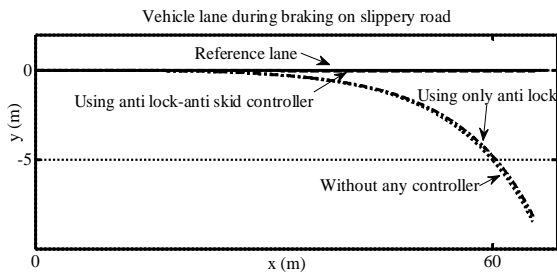

Fig. 12. The vehicle trajectory with/without using a controller.

Another undesirable condition during driving is friction coefficient changes that could take place during the braking time. Therefore, the previous maneuver is repeated using the friction coefficient of Fig. 13.
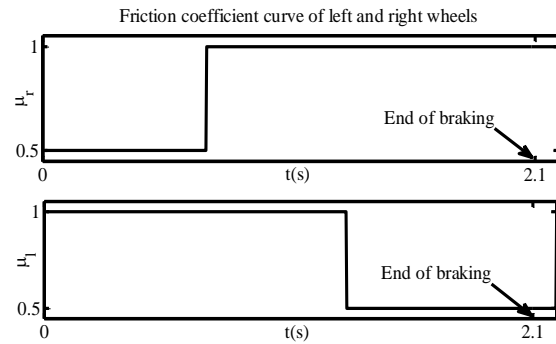

Fig. 13. Friction coefficient changes in left and right wheels during braking.

Figure 14 demonstrates that the anti-lock controller was not capable of preventing vehicle yaw. In contrast to the previous maneuver, the anti-skid controller with an input control of yaw angle was not able to fully maintain the vehicle balance along the desirable trajectory due to changes in friction coefficients during braking. To explain the above point, it is sufficient to review Eqs. (45 and 46) from the third section. As can be seen, yaw angle is calculated from the integration of the vehicle yaw rate. Among the integrator's deficiencies is its prolonged settling time, in that, the integrator cannot estimate the yaw angle in a precise and speedy manner with rapid condition changes. Consequently, the controller cannot operate in a precise manner, and the vehicle is rendered incapable of moving along the desirable trajectory. The provided descriptions, as well as the obtained simulation, results from Fig. 15 point to a superior maintenance of vehicle trajectory when using a yaw rate as a control input.
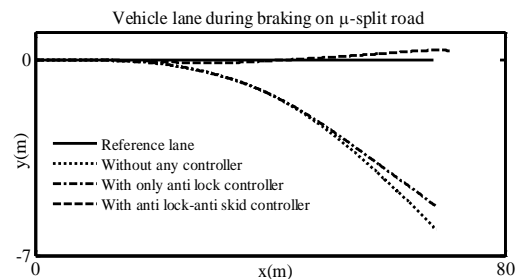

Fig. 14. Vehicle trajectory on a road with different friction coefficients with/without the controller.
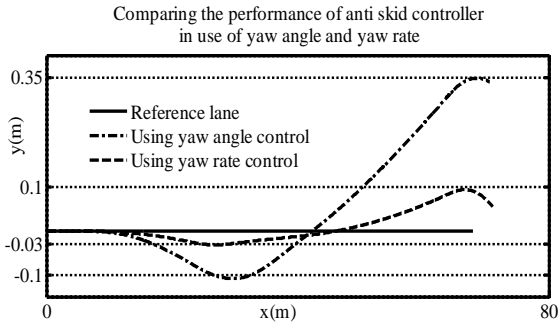
Fig. 15. Comparing the performance of anti-skid controller in use of yaw angle and yaw rate.

4. 2. 2. Hard braking situations on road twists

Another critical condition is hard braking on road twists. In this section, the anti-skid controller performance is evaluated by conducting a single-redirect, as well as double-redirect maneuvers.

4-2-2-1. Single-redirect maneuvers

The following four maneuvers were simulated by applying a fixed steering angle to the vehicle with $\mu_{peak} = 1$ on a dry-asphalt road.

a) Braking with an 18-newton pedal force and a 10-dgeree steering angle, without utilizing any controller.

b) Braking with a 32-newton pedal force and a 10-degree steering angle, without utilizing any controller.

c) Braking with a 32-newton pedal force and a 10-degree steering angle, using anti-lock controller.

d) Braking with a 32-newton pedal force and a 10-degree steering angle, using anti lock-anti skid controller (with yaw angle as control input).

Based on Fig. 16, a soft braking (maneuver A) during a vehicle turn would not lead to any difficulties. Yet, doing the same maneuver with a more intense breaking force (maneuver B) deprives the vehicle of a proper turn, resulting in a phenomenon known as understeer due to locking up the front wheels. As can be seen, anti-lock controller, too, is not capable of improving such situation (maneuver C). However, anti lock-anti skid controller (maneuver D) allows for a proper handling of vehicle and the application of an appropriate steering angle.
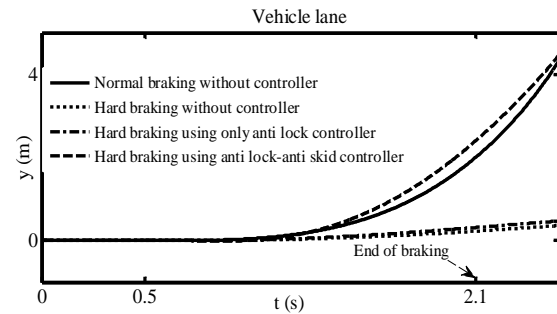

Fig. 16. Comparing normal and hard brakings on road twists with/without using a controller.

In Fig. 17, the curve for wheel braking torque changes is illustrated. The desirable performance of controllers in different moments during braking is evident. As can be seen, despite a similar friction coefficient on the part of the wheels, anti-skid controller was more active in left wheels as a result of a left-hand turn and the subsequent state of slipperiness experienced by left wheels. Anti-lock controller was more active in the front right wheel. In rear wheels, both anti-lock and anti-skid controllers functioned during different times, based on the wheel speed and the vehicle yaw rate.
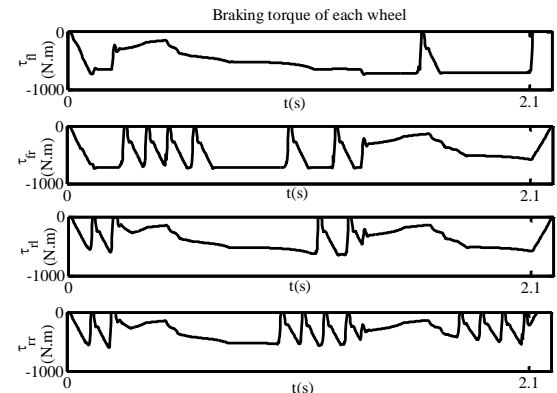

Fig. 17. Wheels torque curves upon braking during turning left.

4. 2. 2. 2. Double-redirect maneuvers

By applying the steering angle in Fig. 18 on a dry-asphalt road and with $\mu_{peak} = 1$, the following four maneuvers were simulated.

Braking with an 8-newton pedal force, without utilizing any controller (the reference trajectory).

Braking with an 18-newton pedal force, without utilizing any controller.

Braking with an 18-newton pedal force, using anti lock-anti-skid controller (with yaw angle as control input).

Braking with an 18-newton pedal force, using anti lock-anti-skid controller (with yaw rate as control input).

The vehicle overall maneuverability is reduced in above speeds, rendering the application of an acute steering angle impossible. As can be seen from Fig. 19, the vehicle was capable of handling a 10-degree steering angle under extremely soft braking conditions, i.e. an 8-newton pedal force. However, should the pedal force increase, not only the vehicle cannot maintain the intended trajectory, but it can lead to vehicle yaw or even overturn. A great vehicle yaw and an eventual overturn for an 18-newton pedal force can be observed. Anti-skid controller with a yaw angle control input improves vehicle trajectory to a great extent, and the performance of an anti-skid controller would be even more enhanced by using a yaw rate control input, drawing the vehicle trajectory nearer to that of the reference. Taking the conducted simulations into account, it is suggested that yaw rate is used in place of yaw angle as control input in anti-skid controllers.

Fig. 18. The steering angle applied to the vehicle.

Fig. 19. The vehicle trajectory during double redirects.

5. Conclusions

Wheel and body simulation with seven degrees of freedom, modeling the vehicle dynamic motion, as well as modeling all parts within a hydraulic braking system, including pedal, the main brake cylinder, wheel brake cylinders, and even modeling the driver's foot pressure on the pedal, allowed for a carefully studying and a reliable designing of an intelligent brake system. This is claimed as one of the strengths of this article compared to other studies. The conducted simulations demonstrate the desirable performance of anti-lock controllers in reducing braking time and distance under hard braking situations. There are two ways to estimate the operation of controllers: a) making a mechanical system and comparing the results with those practical ones that it both takes time and money, or b) examining the controller's operation in critical driving conditions. In a normal situation, it is expected that the vehicle goes without skidding or wheels to be locked. However, the wheels are locked or the vehicle skids, if the friction coefficient reduces on one side of it or a strong braking in the roads curve happens, and its wheels is locked and the controller can manage this condition. The better examination of a controller is when there is an even worse critical condition. Therefore, in stimulation for preparing this paper, the assumption of the sudden reduction of the friction coefficiency of one side of the vehicle or braking with more force on the roads curve makes the condition the best way to estimate the controller. Regarding the performance of anti-skid controllers in maneuvers that do not contain rapid condition changes, it was revealed that it operates favorably with a yaw angle control input. Yet, in maneuvers in which it was faced with rapid condition changes, the yaw angle follows rapid changes with a delay due to prolonged settling time on the part of an integrator (see equations from section 3-3-1-1). Such delay introduced errors in the vehicle trajectory compared to the desirable path. This issue is resolved in controllers with yaw rate control inputs due to a lack of need for an integrator.
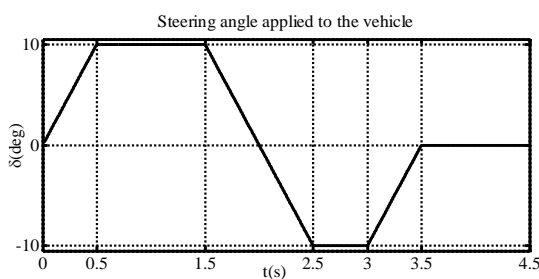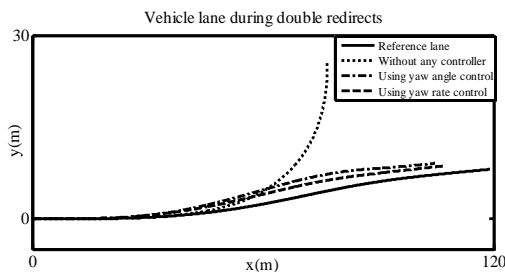
References

[1]   M. J. Gutnecht, D. R. Schniedewend, J. J. Moskwa, C. R. kime and P. Romanathan, "Fault tolerance analysis of alternate automative brake system designs", *SAE Technical paper*, No. 930511, (1993).

[2]   R. H. Madison and H. E. Riordan, "Evolution of the sure track brake system", *SAE Technical paper,* No. 690213, (1969).

[3]   C. Orthwein , "*Clutches and brackes design and selection*" , Marcel Dekker Inc., chapter 12, (2004).

[4]   N. Patra and K. Datta, " *Improved sliding mode controller for anti- lock braking system*", In Proc. CALCON11, pp. 25-30, Kolkata, Nov., (2011).

[5]   A. Harifi, A. Aghagolzadeh, G. Alizadeh, M. Sadeghi, "Designing a sliding mode controller for slip control of antilock brake system", *Transportation Research Part C*, Vol. 16, pp. 731-741, (2008).

[6]   C. Edwards and S. spurgeon, ""*Sliding mode control: Theory and applications*", London, UK: Taylor and francis, (1998).

[7]   V. Utkin, Sliding modes in control and optimization, USA: Springer- Verlag, Berlin, (1992).

[8]   Y. Tang, X. Zhang, D. Zhang, G. Zhao and X. Guan, "Fractional order sliding mode controller design for antilock braking systems" *Jornal of Neurocomputing*, Vol. 111, pp. 122-130, (2013).

[9]   N. Patra and k. Datta , " Sliding mode controller for wheel–slip control of anti-lock braking system", *Proceedings of the Advanced Communication Control and Computing Technologies Conference*, pp. 385-391, Rourkela, India, 23-25 August, (2012).

[10] P. Naderi, S. M. T. Bathaee and A. farhadi, "Driving/regeneration and stability enhancement for a four-wheel-drive hybrid vehicle", *International Review of Electrical Engineering*, Vol. 4, No. 1, (2009)a.

[11] P. Naderi, M. Mirsalim and S. M. T Bathaee, "Driving/regeneration and stability enhancement for a two-wheel-drive electric vehicle", *International Review of Electrical Engineering*, Vol. 4, No. 1, (2009)b.

[12] P. Naderi , A. R. Naderipoar, M. Mirsalim and M. A. fard, "Intelligent braking system using fuzzy logic and sliding mode controller", *Jornal of Control and Intelligent Systems*, Vol. 38, No. 4, pp. 236-244, (2010).

[13] P. Naderi and A. Farhadi, "Non-driven wheels application for intelligent multi-objective control of hibrid vehicles", *International Journal of Robotics and Automation*, Vol. 27, No. 2, pp. 185-197, (2012).

[14] W. Xiany, P. C. Richardson, C. Zhao and S. Mohammad, "Brake-by-wire control system design and analysis", IEE Transaction On Vehicular Technology, Vol. 57, No. 1, PP. 138-147, (2008).

[15] P. Naderi and S. M. sharouni, "Intelligent braking system for stability enhancement of vehicle braking, using fuzzy logic controllers", *International Jornal of Vehicle Safety*, Vol. 6, No. 4, PP. 381-398, (2013).

[16] V. C´irovic´and D. Aleksendric´, "Adaptive neuro-fuzzy wheel slip control", Jornal of Expert Systems with Applications, Vol. 40, pp. 5197-5209, (2013).

[17] R.-E. Precup, et al., "Nature-inspired optimal tuning of input membership functions of takagi-sugeno-kang fuzzy models for anti-lock braking systems", *Appl. Soft Comput. J.* (2014).

[18] M. Wu and M. shih , "Simulated and experimental study of hydranlic anti-lock braking system using sliding mode PWM control" *Jornal of Mechatronics*,Vol. 13, No. 4, pp. 331-351, (2001).

[19] S. Nasiri, B. Moaveni, G. Payganeh and M. Arefiyan "Modeling and analysis of the hydraulic antilock brake system of vehicle ", *Jornal of Control*, Vol. 6, No. 3, pp. 11-26, Fall (2012).

[20] J. H. park, D. H. Kim and Y. J. Kim, "Anti-lock brake system control for buses based on fuzzy logic and a sliding-mode observer ", *International Jornal of KSME*, Vol. 15, No. 10, pp. 1398-1407, (2001).

[21] H. Lin and Ch. Song, "Simulation of hydraulic anti-lock braking system control based on a co-simulation model by AME sim and simulink", *Proceedings of TMEE Conference*, pp. 775-778, Changchun, China, 16-18 December (2011).

[22] M. Kato, T. Matsuto, K. Tanaka, H. Ishihara and W. Hosoda, "Combination of anti-lock brake system (ABS) and combined brake system (CBS) for motorcycles", *SAE*. 960960, pp. 1284-129, (1996).

[23] A. Strichland and K. Dagg, "ABS braking performance and steering input", *SAE Special Publications*, 980240, pp. 57-64, (1998).

[24] F. M. Georg, F. G. Gerard and C. Yann, "Fuzzy logic continuous and quantizing control of an ABS braking system", *SAE*. 940830, pp. 1033-1042, (1994).

[25] N. Miyasaki, M. Fukumoto, Y. Sogo and H. Tsukinoki, "Anti-lock brake system (M-ABS) based on the friction coefficient between the wheel and the

road surface", *SAE special publications,* 900207, pp.101-109, (1990).

[26] C. Y. Lu and M. C. shih "Application of the pacejka magic formula tyre model on a study of a hydraulic anti-lock braking system for a light motorcycle", *Vehicle System Dynamics*, Vol. 6, No. 41, pp. 431-448, (2004).

[27] M. Sugai, H. Yamaguchi, M. Miyashita, T. Umeno and K. Asano , "new control technique for maximizing braking force on anti- lock braking system", *Vehicle System Dynamics*, No. 32, pp. 229-312, (1999).

[28] Ch. K. Huang and M. Ch. Shih , "Design of a hydraulic anti–lock braking system (ABS) for a motorcycle", *Journal of Mechanical Science and Technology*, Vol. 5, No. 24, pp. 1141-1149, (2010).

[29] B. Wang, et al., "a Robust wheel slip ratio control design combining hydraulic and regenerative braking systems for in-wheel-motors-driven electric vehicles", *Journal of the Franklin Institute*, (2014).

[30] H. Mirzaeinejad, M. Mirzaei, "Optimization of nonlinear control strategy for anti-lock braking system with improvement of vehicle directional stability on µ -split roads", *Jornal of Transportation Research Part C*, Vol. 46, pp. 1-15, (2014).

Attachments

The simulated vehicle's specifications.

Definition	Symbol	Unit	Amount
Brake fluid density	ρ_0	Kg/m^3	1027
The maximum cross section of oil tubes	A_0	m^2	1.2×10^{-8}
Liquid bulk modulus	β	N/m^2	6.9×10^5
The main cylinder cross section	A_{mc}	m^2	2.85×10^{-4}
Damping coefficient	C	Nm/s	100
Wheel cylinder cross section	A_w	m^2	1.8×10^{-4}
The main cylinder initial volume	V_{mc0}	m^3	2.85×10^{-7}
Wheel cylinder initial volume	V_{w0}	m^3	5.4×10^{-7}
Cylinder spring stiffness	K	N/m	50
Orifice coefficient	C_d	__	0.001
Brake oil coefficient	ρ_0	Kg/m^3	1027
The maximum cross section of oil pipe	A_0	m^2	1.2×10^{-8}

Liquid bulk modulus	β	N/m^2	6.9×10^5
The cross section of the master cylinder	A_{mc}	m^2	2.85×10^{-4}
Damping coefficient	C	Nm/s	100
The cross section of the wheel cylinder	A_w	m^2	1.8×10^{-4}
The initial volume of the main cylinders	V_{mc0}	m^3	2.85×10^{-7}
Cylinder spring stiffness	K	N/m	50
Damping coefficien	C_d	__	0.001
Vehicle's total mass	M_t	kg	850
The distance from the front axis to the center of gravity	L_f	m	1.147
The distance from the rear axis to the center of gravity	L_r	m	1.197
Vehicle inertia around the z-axis	I_z	$Kg.m^2$	1800
Wheel longitudinal stiffness	C_x	N	17500
Wheel lateral stiffness	C_y	N/rad	15000
The center of gravity height	h_{cg}	m	0.5
The length of vehicle axes	T_a	m	1.4
The wheel radius	R_w	m	0.275
The wheel inertial	I_w	$Kg.m^2$	3.2639